Biochem. J. (2012) **443**, 173–183 (Printed in Great Britain) doi:10.1042/BJ20112078

The guanine-nucleotide-exchange factor P-Rex1 is activated by protein phosphatase 1α

Mark A. BARBER*, Annick HENDRICKX†, Monique BEULLENS†, Hugo CEULEMANS†, David OXLEY‡, Sylvia THELEN§, Marcus THELEN§, Mathieu BOLLEN† and Heidi C. E. WELCH*[1]

*Inositide Programme, Babraham Institute, Cambridge, U.K., †Department of Molecular Cell Biology, Catholic University Leuven, Leuven, Belgium, ‡Proteomics Group, Babraham Institute, Cambridge, U.K., and §Institute for Research in Biomedicine, Bellinzona, Switzerland

P-Rex1 is a GEF (guanine-nucleotide-exchange factor) for the small G-protein Rac that is activated by PIP_3 (phosphatidylinositol 3,4,5-trisphosphate) and G$\beta\gamma$ subunits and inhibited by PKA (protein kinase A). In the present study we show that PP1α (protein phosphatase 1α) binds P-Rex1 through an RVxF-type docking motif. PP1α activates P-Rex1 directly *in vitro*, both independently of and additively to PIP_3 and G$\beta\gamma$. PP1α also substantially activates P-Rex1 *in vivo*, both in basal and PDGF (platelet-derived growth factor)- or LPA (lysophosphatidic acid)-stimulated cells. The phosphatase activity of PP1α is required for P-Rex1 activation. PP1β, a close homologue of PP1α, is also able to activate P-Rex1, but less effectively. PP1α stimulates P-Rex1-mediated Rac-dependent changes in endothelial cell morphology. MS analysis of wild-type P-Rex1 and a PP1α-binding-deficient mutant revealed that endogenous PP1α dephosphorylates P-Rex1 on at least three residues, Ser^{834}, Ser^{1001} and Ser^{1165}. Site-directed mutagenesis of Ser^{1165} to alanine caused activation of P-Rex1 to a similar degree as did PP1α, confirming Ser^{1165} as a dephosphorylation site important in regulating P-Rex1 Rac-GEF activity. In summary, we have identified a novel mechanism for direct activation of P-Rex1 through PP1α-dependent dephosphorylation.

Key words: dephosphorylation, guanine-nucleotide-exchange factor (GEF) P-Rex1, mechanism of regulation, P-Rex family, serine/threonine protein phosphatase PP1, small G-protein (GTPase) Rac.

INTRODUCTION

The Rac family of small G-proteins are essential controllers of actomyosin cytoskeletal structure (and hence cell shape, adhesion, motility, phagocytosis and regulated secretion), gene expression and ROS (reactive oxygen species) formation [1]. Among the four Rac isoforms, Rac1 is ubiquitous and essential for development, Rac2 haemopoietic, Rac3 neuronal and RhoG widely distributed. Rac is tightly regulated through activation by GEFs (guanine-nucleotide-exchange factors), which outnumber it by approximately 20:1, and inhibition by GTPase-activating proteins.

The P-Rex family of Rac-GEFs comprises P-Rex1 [2], P-Rex2 [3] and the splice variant P-Rex2b [4]. They are 185 kDa proteins containing a catalytic DH and tandem PH domain, two pairs of DEP and PDZ domains, and a C-terminal half (truncated in P-Rex2b) that is homologous with IP4P (inositol polyphosphate-4-phosphatase). P-Rex1 is mainly expressed in leucocytes, brain, spleen and lymph nodes [2,5,6], P-Rex2 in cerebellar Purkinje neurons and the lung [3,5], and P-Rex2b in the heart and endothelial cells [4,7]. P-Rex family GEFs activate Rac1, Rac2 and Rac3 *in vivo*, with isoform preference depending on the cell type [8–11]. Through Rac, they control GPCR (G-protein-coupled receptor)-dependent ROS production, adhesion and chemotaxis of phagocytes [8–12], GPCR-dependent migration of endothelial cells [7,13,14], and GPCR- or neurotrophin-dependent morphology and chemotaxis of neurons [5,6,11,15]. P-$Rex1^{-/-}$ mice show reduced neutrophil recruitment to inflammatory sites [10] and impaired melanocyte migration during development [16], whereas P-$Rex2^{-/-}$ and P-$Rex1^{-/-}$/P-$Rex2^{-/-}$ mice have defects in the dendrite morphology and synaptic plasticity of Purkinje neurons and in motor functions [5,15]. P-Rex family GEFs are also currently emerging as important in cancer progression and metastasis. P-Rex1 expression is significantly increased in prostate cancer, breast cancer and melanoma, correlates with metastatic potential, and affects the migration and invasiveness of cancer cells [16–19]. Grafts of P-Rex1-expressing cells promote prostate cancer metastasis and breast tumour growth in mice [17–19], and P-$Rex1^{-/-}$ mice show a drastic reduction in melanoma metastasis [16]. P-Rex2 is one of the most frequently mutated Rho-GEFs in cancer and shows increased expression in a range of cancer types. It inhibits the activity of the tumour suppressor PTEN, and its overexpression with constitutively active PI3K (phosphoinositide 3-kinase) confers growth-factor independent proliferation to breast cancer cells [20]. In summary, P-Rex family GEFs are important regulators of Rac-dependent processes elicited by stimulation of GPCRs and/or PI3K-coupled receptors, such as ROS production in phagocytes, and morphology changes and migration of a range of cell types, including phagocytes, neurons and cancer cells.

The P-Rex family GEFs differ from other Rac GEFs in their mode of regulation. They are directly and synergistically activated *in vitro* and *in vivo* by the lipid second messenger PIP_3 (phosphatidylinositol 3,4,5-trisphosphate), which is generated by class 1 PI3K, and by the G$\beta\gamma$ subunits of heterotrimeric

Abbreviations used: CRIB, Cdc42 (cell-division cycle 42)/Rac-interacting binding; DMEM, Dulbecco's modified Eagle's medium; DTT, dithiothreitol; EE, Glu–Glu tag; eIF2β, eukaryotic initiation factor 2β; FBS, fetal bovine serum; GEF, guanine-nucleotide-exchange factor; GFP, green fluorescent protein; eGFP, enhanced GFP; GPCR, G-protein-coupled receptor; GST, glutathione transferase; HEK, human embryonic kidney; IP4P, inositol polyphosphate-4-phosphatase; LC–MS/MS, liquid chromatography tandem MS; LPA, lysophosphatidic acid; PAE, porcine aortic endothelial; Pak, p21-activated kinase; PDGF, platelet-derived growth factor; PI3K, phosphoinositide 3-kinase; PIP_3, phosphatidylinositol 3,4,5-trisphosphate; PK, protein kinase; PP1, protein phosphatase 1; ROS, reactive oxygen species; siRNA, small intefering RNA; WT, wild-type.

[1] To whom correspondence should be addressed (email heidi.welch@babraham.ac.uk).

G-proteins, which are released upon stimulation of GPCRs [2,3,21]. This dual mode of regulation makes P-Rex family GEFs ideal coincidence detectors for the concomitant activation of PI3K and GPCRs. Synergy of PIP_3 and $G\beta\gamma$ subunits is also required for P-Rex1 translocation to the plasma membrane [22]. PIP_3 binds to and activates P-Rex1 through the PH domain, and $G\beta\gamma$ subunits activate P-Rex1 through the DH domain [21]. A range of different $G\beta$ and $G\gamma$ combinations, with the exception of $G\beta_5\gamma_2$, can activate P-Rex1 [23]. *In vivo*, the interaction with $G\beta\gamma$ involves the second DEP domain, and first PDZ and IP4P domains of P-Rex1 [24], whereas *in vitro*, the isolated DH domain is sufficient for stimulation of P-Rex1 activity by $G\beta\gamma$ [21,22]. The DEP, PDZ and IP4P domains help to keep the catalytic activity of full-length P-Rex1 low and keep it localized to the cytosol in resting cells, suggesting that P-Rex1 is auto-inhibited by intra-molecular interactions between the DH/PH tandem and these domains in its basal state [21,22]. P-Rex family GEFs are also regulated through phosphorylation. Cyclic AMP-dependent kinase A [PK (protein kinase) A] inhibits PIP_3- and $G\beta\gamma$-dependent P-Rex1 activity *in vitro*, and PI3K- or GPCR-dependent P-Rex1 activity *in vivo* [25]. PKA also inhibits P-Rex1 membrane translocation in neutrophils [26]. However, the serine/threonine phosphatase(s) that reverse the inhibition of P-Rex1 by PKA remain to be identified. Although PKA is currently the only kinase known to interact directly with P-Rex1, several others have been shown to affect P-Rex1 *in vivo*. P-Rex1 membrane translocation is sensitive to tyrosine kinase inhibitors [26], and P-Rex1-dependent ROS formation in COS^{phox} cells is increased by co-expression of PKB or PKCδ [27]. In breast cancer cells, P-Rex1 is phosphorylated on four serine residues (Ser^{313}, Ser^{319}, Ser^{605} and Ser^{1169}) whose phosphorylation state is affected by stimulation of receptor-tyrosine kinases, through unidentified serine kinases and phosphatases [17].

The PP1 (protein phosphatase 1) family consists of three 35–38 kDa isoforms, PP1α, PP1β (also called δ) and PP1γ, which are ubiquitously expressed, highly conserved and estimated to catalyse one-third of all protein dephosphorylations [28]. Like other serine/threonine phosphatases, they are constitutively active catalytic subunits regulated through obligatory holoenzyme formation with other proteins [29]. Typical PP1-interacting proteins contain an 'RVxF' binding motif, more accurately defined as [RK]-$X_{(0,1)}$-[VI]-Ψ-[FW], where X is any residue and Ψ is any residue except proline [30]. Currently, approximately 180 PP1-interacting proteins are known, although only a small number have been characterized [31]. Of these, the majority regulate the subcellular localization and/or inhibit the phosphatase activity of PP1, but only a minority are themselves targets of PP1-mediated dephosphorylation [28,32]. In a screen of RVxF motif-containing proteins, we have found that a fragment of P-Rex2 can bind PP1 [31]. In the present paper, we investigated whether full-length P-Rex family GEFs are able to interact with PP1 and whether this interaction has an influence on GEF function.

EXPERIMENTAL

Constructs

The fragment P-Rex2-(983–1187) (human) was cloned into pET160-DEST for bacterial expression using the Gateway system (Invitrogen). Mammalian expression vectors pCMV3(EE)-P-Rex1 WT (wild-type) and pCMV3(Myc)-P-Rex1 WT for full-length human P-Rex1 [2], and pGEX-2TK-PP1α for bacterial expression of GST (glutathione transferase)–PP1α [31], have been described previously. The mutants P-Rex1 V1147A/F1149A (VAFA), P-Rex1 S1165A and 'cluster' (S1165A, S1182A, S1169A, S1179A and S1185A) were generated by site-directed mutagenesis. P-Rex1 VAFA was derived from full-length human P-Rex1 WT in pBSII-SK + using the primers 5′-GGGGGCAT-CAAGAAGGCGTGCGCCAAGGTGGCCGAGGAGG-3′ and 5′-CCTCCTCGGCCACCTTGGCGCACGCCTTCTTGATGCC-CCC-3′ (mutated residues underlined), and subcloned into pCMV3 [Myc or EE (Glu–Glu tag)] by inserting a 588 bp MfeI/NruI restriction fragment into MfeI/NruI-digested pCMV3 (Myc or EE) P-Rex1 WT. Phosphatase-dead PP1α R96A, a gift from Professor Angus Nairn (Yale University, New Haven, CT, U.S.A.), was subcloned into pEGFP-C1 (Clontech) by inserting an XmaI/AflII fragment into XmaI/AflII-cut pEGFP-C1-PP1α WT.

Recombinant proteins

His–P-Rex2-(983–1187), His–eIF2β (eukaryotic initiation factor 2β)-(1–144) and His–eIF2β-(1 – 144) (mut) were expressed in *Escherichia coli* BL21(DE3)pLysS (Stratagene) and purified using Ni^{2+}–Sepharose [33]. GST–PP1α was expressed in *E. coli* BL21(DE3)pLysS (Stratagene), purified with glutathione–Sepharose 4B (GE Healthcare) and eluted with 10 mM reduced L-glutathione (pH 7.5; Sigma) in 150 mM NaCl, 50 mM Tris/HCl (pH 8.0), 1 mM EGTA and 1 % Triton X-100. Purified native P-Rex1 from pig neutrophils and purified Sf9-cell-derived human full-length $G\beta\gamma$ subunits (EE–$\beta_1\gamma_2$), EE–P-Rex, EE–Rac1 and EE–Rac2 were prepared as described previously [2,21,34]. Native PP1 was purified from rabbit skeletal muscle as described previously and was a mixture of all three isoforms [35]. Recombinant rabbit PP1α was from Calbiochem.

Cell culture

PAE (porcine aortic endothelial) cells which stably overexpress the PDGF (platelet-derived growth factor) β receptor [36] were cultured in Ham's F12 Nutrient mixture (Gibco), 10 % FBS (fetal bovine serum), 100 units/ml penicillin and 1 mg/ml streptomycin at 37 °C in 5 % CO_2. COS-7 and HEK (human embryonic kidney)-293 cells [both from A.T.C.C. (Manassas, VA, U.S.A.)] were cultured in DMEM (Dulbecco's modified Eagle's medium; Gibco), 10 % FBS, 100 units/ml penicillin and 1 mg/ml streptomycin at 37 °C in 5 % CO_2. All cells were passaged by tryptic digest approximately every 2 days and used after between 1 and 12 weeks in culture.

Western blotting

Primary antibodies were all monoclonal. Anti-EE, -Myc and -GST tag antibodies were from the Babraham Monoclonal Antibody Unit (Cambridge, U.K.). The anti-P-Rex1 antibody was 6F12 [2]. The anti-Rac1 antibody was from Millipore (catalogue number 05-389); the anti-PP1α (catalogue number P7607) and -phosphoserine (catalogue number P3430) antibodies were from Sigma; and the anti-PP1β antibody (catalogue number ab16369) was from Abcam. Secondary antibodies were HRP (horseradish peroxidase)-coupled IgG from Bio-Rad Laboratories. Proteins were detected by ECL (enhanced chemiluminesence; Amersham). When required, membranes were stripped in 25 mM glycine (pH 2.0) and 1 % SDS for 30 min at 22 °C before reprobing. Densitometric scanning was done using ImageJ software (http://rsbweb.nih.gov/ij/).

Protein-binding assays

Bacterially expressed His–P-Rex2-(983–1187) and Sf9-cell-derived purified human EE–P-Rex1 and EE–P-Rex2 were subjected to PP1α-binding and phosphorylase phosphatase activity assays as described previously [31,37]. For binding assays

with His–P-Rex2-(983–1187), equimolar amounts of GST and GST–PP1α were preincubated for 1 h at 10 °C with glutathione agarose prior to the addition of His–P-Rex2-(983–1187) for 1 h and analysis of precipitates by SDS/PAGE and Western blotting. For binding assays with native P-Rex1, 50 pmol of GST or GST–PP1α were incubated with 8 pmol of native pig-neutrophil-derived purified P-Rex1 for 1.5 h at 4 °C, before pull down with glutathione–Sepharose, washing (in PBS, 1 % Triton X-100, 5 mM EGTA, 1 mM EDTA, 25 mM NaF and 20 mM 2-glycerophosphate) and analysis by SDS/PAGE (8 % gel) and Western blotting.

Co-immunoprecipitation assays

COS-7 cells were transfected by electroporation with pEGFP-PP1α and/or pCMV3(Myc)-P-Rex1 (and empty pCMV3 or pEGFP where appropriate), cultured for 30 h and then serum-starved in DMEM and 0.5 % FAF (fatty-acid free)-BSA for 14 h. Cells were scraped into lysis buffer [150 mM NaCl, 20 mM Hepes (pH 7.2 at 4 °C), 1 mM EDTA, 5 mM EGTA, 1 mM DTT (dithiothreitol), 0.1 mM PMSF, and 10 μg/ml each of leupeptin, pepstatin-A, aprotinin and antipain) and probe sonicated. Lysates were cleared at 12 000 **g** for 5 min at 4 °C (aliquots of total lysate removed at this point) and incubated with anti-GFP (green fluorescent protein) antibody (catalogue number G6539, Sigma) for 1.5 h on ice before the addition of Protein A–Sepharose for 30 min. Precipitates were washed and analysed by SDS/PAGE (8 % gel) and Western blotting alongside total lysate controls. Co-immunoprecipitation of endogenous proteins was performed using a similar protocol, except that HEK-293 cells were used.

In vitro Rac-GEF activity assay with PP1α pre-treatment

Liposome-based *in vitro* assays for P-Rex1 Rac-GEF activity were performed with purified recombinant EE–Rac2, EE–P-Rex1, G$\beta\gamma$ subunits (EE–$\beta_1\gamma_2$) and stearoyl-arachidonoyl-PIP_3 as described previously [2,21,22], except for the following adaptation to measure the effects of PP1α: 100 nM P-Rex1 [in 20 mM Hepes (pH 7.0 at 4 °C), 10 % ethylene glycol, 1 % betaine, 0.01 % sodium azide, 0.5 mM EGTA and 0.2 M KCl] was incubated for 30 min at 30 °C with purified native rabbit PP1 (100 nM final assay concentration) or recombinant PP1α (160 nM final assay concentration) in an equal volume of PP1α dilution buffer [50 mM Hepes (pH 7.0), 50 % glycerol, 0.1 mM EGTA, 1 mM $MnCl_2$, 2.5 mM DTT and 0.025 % Tween 20], or with buffer alone. In assays with okadaic acid (Calbiochem), the inhibitor was added to 0.5 μM both during pre-incubation and GEF assay.

Pak (p21-activated kinase)-CRIB [Cdc42 (cell-division cycle 42)/Rac-interacting binding] Rac activity assays

HEK-293 cells were plated on to 9-cm dishes and transfected the following day with P-Rex1 and/or PP1α plasmids (or empty vectors as appropriate) using JetPEI (Polyplus). At 42 h later, the cells were serum-starved in FBS-free medium for 5 h. In some experiments, cells were then stimulated with 50 nM LPA (lysophosphatidic acid; Sigma) or mock-treated, for 1 min. Medium was aspirated, the dishes chilled and cells scraped into ice-cold buffer [10 % glycerol, 50 mM Tris/HCl (pH 7.4), 100 mM NaCl, 1 % Nonidet P40 and 2 mM $MgCl_2$] and lysed on ice for 4 min with occasional vortex mixing. Lysates were cleared at 12 000 ***g*** for 5 min at 4 °C (total lysate aliquots taken at this point) and incubated for 15 min at 4 °C with GST–Pak-CRIB [38] precoupled to glutathione–Sepharose. Beads were washed, and protein analysed by SDS/PAGE and Western blotting. In some experiments, expression of endogenous PP1α was reduced by siRNA (small interfering RNA) (CCGCATCTATGGTTTCTAC; Dharmacon), or non-targeting siGENOME siRNA (Dharmacon) used as control, by addition to JetPEI transfections at 25 nM and incubating the cells for 48 h before Pak-CRIB assays.

Cell morphology assays

PAE cells were transfected by electroporation with P-Rex1 and/or PP1α plasmids (or empty vectors as appropriate) or with V12-Rac, and plated on to sterile glass coverslips. After 16 h in antibiotic-free medium, cells were starved in serum-free medium for 6 h. Cells were then stimulated for 5 min with 10 ng/ml PDGF (or mock-treated), washed, fixed with 4 % paraformaldehyde [in 100 mM Pipes (pH 7.2 with KOH), 2 mM EGTA and 2 mM $MgCl_2$], and permeabilized in PBS with 0.2 % Triton X-100 before staining with anti-Myc antibody and Alexa Fluor® 568 goat anti-(mouse IgG) (Molecular Probes). Coverslips were mounted in Aqua Polymount (PolySciences) and the cells were analysed for P-Rex1 and PP1α expression and their morphology on a Zeiss Axiophot 2 microscope with a SPOT camera (Diagnostic Instruments Inc) using a 60× oil-immersion objective. Scoring was done blindly.

Identification of phosphorylation sites by LC–MS/MS (liquid chromatography tandem MS)

EE–P-Rex1 WT and EE–P-Rex1 VAFA were overexpressed in PAE cells by electroporation. At 48 h after transfection, EE-tagged proteins were immunoprecipitated from cell lysates with anti-EE–Sepharose and subjected to SDS/PAGE and Coomassie Blue staining. P-Rex1 bands were excised and destained with 25 mM ammonium bicarbonate/50 % acetonitrile. Destained proteins were reduced, carbamidomethylated and digested overnight with 10 μg/ml sequencing grade proteases (Promega) in 25 mM ammonium bicarbonate (pH 8.2) at 30 °C. Portions of the slices were digested separately with three different proteases (trypsin, chymotrypsin and AspN) to achieve 96 % sequence coverage. Phosphopeptides were extracted from the digests with Fe^{3+}-loaded IMAC (immobilized metal-ion-affinity chromatography) beads (Phos-Select, Sigma) and separated by reverse-phase liquid chromatography (column size = 0.05 mm × 100 mm, Vydac C18 with 5 μm particle size), with an acetonitrile gradient (10–40 % over 30 min) containing 0.1 % formic acid, at a flow rate of 150 nl/min. The column was coupled to a nanospray ion source (Protana Engineering) fitted to a quadrupole-TOF (time-of-flight) mass spectrometer (Qstar Pulsar I, Applied Biosystems/MDS Sciex), operating in information-dependent acquisition mode. Mass spectral data were searched against the human entries in the Uniprot database and all putative phosphopeptide identifications were verified by manual interpretation of the corresponding LC–MS/MS spectra. Phosphorylation differences between P-Rex1 WT and P-Rex1 VAFA were quantified by measuring the ratios of the peak areas of the extracted-ion-chromatograms of the phosphopeptide pseudomolecular ions between the two samples, relative to the corresponding non-phosphorylated peptides.

RESULTS

P-Rex1 and P-Rex2 bind PP1α

We previously found that a fragment of P-Rex2 consisting of residues 983–1187, which contains an RVxF PP1-binding motif, can bind PP1 [31]. In the present study, we first tested the specificity of this interaction by comparing His–P-Rex2-(983–1187) binding to GST–PP1α and GST. The P-Rex2 fragment bound GST–PP1α, but not GST (Supplementary Figure S1A

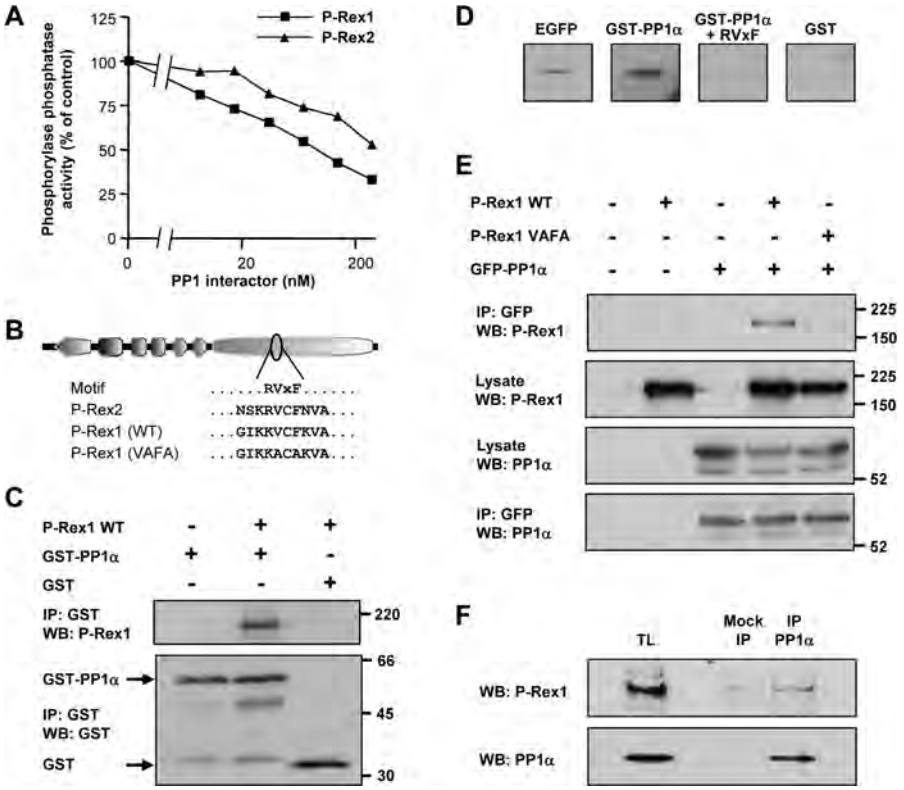

Figure 1 P-Rex1 and P-Rex2 are PP1α-binding proteins

(**A**) Dose-dependent inhibition of the phosphorylase phosphatase activity of purified rabbit PP1 by purified Sf9-cell-derived full-length human EE–P-Rex1 and EE–P-Rex2. Results are means $\pm$ S.E.M. ($n = 3$). (**B**) Schematic representation of the RVxF motif in P-Rex1 and P-Rex2 and its mutation in P-Rex1 VAFA. (**C**) Binding of native P-Rex1 to GST–PP1α. Equimolar amounts of GST–PP1α or GST were incubated with purified native pig P-Rex1 prior to pull down with glutathione–Sepharose, SDS/PAGE and Western blotting (WB) with anti-P-Rex1 and -GST antibodies. Molecular mass markers are given in kDa on the right-hand side. (**D**) Far-Western: immunoprecipitated eGFP–P-Rex1 (full-length) was subjected to SDS/PAGE and Western transfer. The membrane was cut into strips which were incubated separately with GST–PP1α in the presence or absence of excess RVxF peptide, or with GST, as indicated, and then together with anti-GST antibody. The strip in the left-hand panel was incubated with anti-GFP antibody. (**E**) P-Rex1 forms a complex with PP1α *in vivo* which is disrupted by mutation of the RVxF motif. Lysates of COS-7 cells expressing EE–P-Rex1 WT, EE–P-Rex1 VAFA and/or eGFP–PP1α were subjected to immunoprecipitation with an anti-GFP antibody. Western blot analysis of precipitates and total lysates were performed with anti-P-Rex1 and anti-PP1α antibodies. Blots shown are from one experiment and representative of three. Molecular mass markers are given in kDa on the right-hand side. (**F**) Endogenous P-Rex1 forms a complex with endogenous PP1α *in vivo*. HEK-293 cell lysates were subjected to immunoprecipitation with an anti-PP1α antibody. Western blots of precipitates and total lysates (TL) were performed using anti-P-Rex1 and -PP1α antibodies. Blots shown are from one experiment and representative of four. IP, immunoprecipitation.

at http://www.BiochemJ.org/bj/443/bj4430173add.htm). It bound PP1 activity to a similar degree as did eIF2β-(1–144), a known PP1 interactor, unlike eIF2β-(1–144) with a mutated RVxF motif (mut) which did not (Supplementary Figure S1B). As most PP1-interacting proteins inhibit the constitutive catalytic activity of the phosphatase [32], we tested whether this was also the case for P-Rex2. Indeed, the P-Rex2 fragment inhibited PP1 activity *in vitro* to a similar degree as eIF2β-(1–114) ($IC_{50} \sim 500$ nM); full-length P-Rex2 was even more effective than the fragment ($IC_{50} \sim 200$ nM), whereas eIF2β-(1–114) (mut) again had no effect (Figure 1A and Supplementary Figure S1C).

The RVxF-type PP1-docking motif is highly evolutionarily conserved between the full-length members of the P-Rex family (Figure 1B and Supplementary Figure S1D). Hence it seemed plausible that the interaction with PP1 is conserved between P-Rex1 and P-Rex2. Indeed, full-length P-Rex1 also inhibited PP1 activity, to a slightly greater extent than P-Rex2 ($IC_{50} \sim 50$ nM) (Figure 1A). The known mechanisms of regulation are very similar between different members of the P-Rex family, but most previous characterization work has been done on P-Rex1, so we focused on the interaction of P-Rex1 with PP1 from this point onwards. We tested binding of native P-Rex1 to PP1α. Purified native P-Rex1 from pig neutrophils bound to purified recombinant bacterial GST–PP1α, but not GST, suggesting that the interaction between P-Rex1 and PP1α is direct and independent of additional proteins (Figure 1C). We confirmed this by far-Western analysis of eGFP (enhanced GFP)–P-Rex1 binding to GST–PP1α. eGFP–P-Rex1 bound to GST–PP1α, but not GST, and could be competed off with a synthetic RVxF-containing decapeptide, indicating that direct PP1α binding to P-Rex1 is mediated through the RVxF motif (Figure 1D).

To investigate whether P-Rex1 and PP1α interact *in vivo*, we overexpressed eGFP–PP1α and EE–P-Rex1 in COS-7 cells and analysed anti-GFP immunoprecipitates by Western blotting. EE–P-Rex1 co-immunoprecipitated with eGFP–PP1α, suggesting that P-Rex1 and PP1α interact *in vivo* (Figure 1E). To test the RVxF motif-dependence of this interaction, we generated a P-Rex1 mutant with two amino acid substitutions in the RVxF motif (V1147A and F1149A, termed P-Rex1 VAFA). Equivalent substitutions disrupt the interaction between PP1 and other binding partners [37,39]. In contrast with WT EE–P-Rex1, EE–P-Rex1 VAFA did not co-immunoprecipitate with eGFP–PP1α, showing that the RVxF motif confers the interaction between P-Rex1 and PP1α *in vivo* (Figure 1E). To investigate whether endogenous P-Rex1 and PP1α also interact, we precipitated PP1α from HEK-293 cells and analysed co-immunoprecipitation of P-Rex1. Endogenous P-Rex1 co-immunoprecipitated with endogenous PP1α, suggesting that P-Rex1 and PP1α interact *in vivo* at

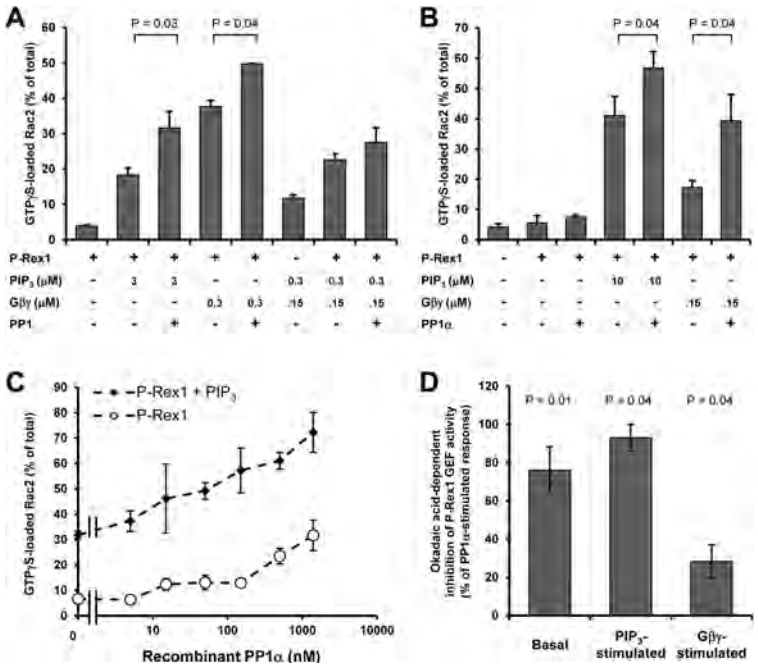

Figure 2 PP1α stimulates P-Rex1 Rac-GEF activity *in vitro*

(**A**) Native rabbit PP1 activates P-Rex1 *in vitro*. The Rac2-GEF activity of Sf9-cell-derived purified human EE–P-Rex1 was assayed with the indicated concentrations of stearoyl-arachidonoyl-PIP_3 and/or $G\beta_1\gamma_2$ after a 30 min pre-incubation of P-Rex1 in the presence or absence of 100 nM native rabbit PP1. Results are means ± range from one experiment and representative of three. Significance was determined using Student's *t* test. (**B**) Recombinant PP1α stimulates the basal, PIP_3- and G$\beta\gamma$-dependent P-Rex1 GEF activities *in vitro*. P-Rex1 Rac2-GEF activity was assayed with the indicated concentrations of PIP_3 or G$\beta\gamma$ after a 30 min pre-incubation with or without 160 nM recombinant *E. coli*-derived PP1α. Results are means ± range or S.E.M., as appropriate, of two basal, three PIP_3 and four G$\beta\gamma$ experiments. Significance was determined using Student's *t* test.. (**C**) PP1α dose-dependently stimulates P-Rex1 Rac-GEF activity. P-Rex1 Rac-GEF activity was assayed in the presence or absence of 10 μM PIP_3 and the indicated concentrations of recombinant PP1α. Basal and PIP_3-dependent activities were measured with 50 nM and 10 nM P-Rex1 respectively to be within the linear range of the assay. Results are means ± range or S.E.M., as appropriate, of two basal and three PIP_3 experiments. (**D**) PP1α stimulation of P-Rex1 requires phosphatase activity. *In vitro* assays were performed as in (**B**) in the presence of 0.5 μM okadaic acid. Results are means of two basal, three PIP_3 and four G$\beta\gamma$ experiments, presented as the percentage inhibition of PP1α-dependent P-Rex1 activity. Significance was determined using a Student's *t* test.

physiological levels (Figure 1F). Taken together, the *in vitro* and *in vivo* data suggest that full-length P-Rex1 and P-Rex2 directly interact with PP1α via the RVxF motif in their IP4P domain.

PP1α activates P-Rex1 Rac-GEF activity *in vitro*

We tested whether PP1α affects P-Rex1 Rac-GEF activity *in vitro* using recombinant Sf9-cell-derived EE–P-Rex1 and EE–Rac2, and purified native rabbit PP1. PP1 stimulated the PIP_3-dependent Rac-GEF activity of an equimolar concentration of EE–P-Rex1 by 70 % and the G$\beta\gamma$-dependent P-Rex1 activity by 30 % (Figure 2A). Therefore native purified PP1 directly stimulates P-Rex1 Rac-GEF activity, although its impact may differ slightly between PIP_3- and G$\beta\gamma$-dependent responses. There was also a tendency for a modest PP1-dependent increase when P-Rex1 was co-stimulated with sub-maximal concentrations of both G$\beta\gamma$ and PIP_3 (Figure 2A).

Since the native PP1 preparation is a mixture of all three isoforms, we next conducted similar experiments with purified recombinant *E. coli*-expressed PP1α. Recombinant PP1α stimulated the basal EE–P-Rex1 Rac-GEF activity by 30 % and the PIP_3- and G$\beta\gamma$-dependent activities by 40 % and 130 % respectively (Figure 2B). Furthermore, the basal Rac1-GEF activity of EE–P-Rex1 was stimulated by PP1α in a similar way as its Rac2-GEF activity (Figure 2B and Supplementary Figure S1E). Thus bacteria-derived PP1α can activate P-Rex1, which shows that, among PP1 isoforms, at least PP1α can activate P-Rex1 and that post-translational modification of PP1α is not required. The slightly different extent to which recombinant and native PP1 activate P-Rex1 probably reflects the variations in PIP_3 and G$\beta\gamma$ concentrations we used to keep Rac activity within the linear range in both assays.

Recombinant PP1α stimulated both the basal and PIP_3-dependent P-Rex1 Rac2-GEF activities in a dose-dependent manner. At the highest concentration of PP1α tested (1.4 μM), basal P-Rex1 activity was stimulated 5.2-fold and PIP_3-dependent activity 2.3-fold (Figure 2C). Both dose–response curves ran approximately in parallel, suggesting additive effects of PP1α and PIP_3 on P-Rex1 activity. Interestingly, the curves did not reach saturation even at higher concentrations where PP1α was present in molar excess. This indicates perhaps that PP1α acts on several target sites sequentially (at least *in vitro*), each event stimulating P-Rex1 further. In summary, PP1α directly stimulates P-Rex1 Rac-GEF activity *in vitro*, both independently of and additively to, PIP_3 or G$\beta\gamma$.

We next tested whether phosphatase activity is required for the activation of P-Rex1 by PP1α. We performed *in vitro* Rac-GEF activity assays in the presence of okadaic acid, a potent phosphatase inhibitor that does not affect PP1 binding to the RVxF docking motif [40,41]. Okadaic acid inhibited PP1α stimulation of the basal and PIP_3-dependent Rac-GEF activities of EE–P-Rex1 by 76 % and 93 % respectively (Figure 2D). Thus the phosphatase activity of PP1α is important for activation of P-Rex1, suggesting that PP1α activates P-Rex1 by dephosphorylation. Interestingly, okadaic acid did not completely eliminate PP1α stimulation of P-Rex1 activity. In particular, the G$\beta\gamma$-dependent response was less sensitive (28 % reduction). Hence although phosphatase activity is a major factor, complex formation (and perhaps conformational

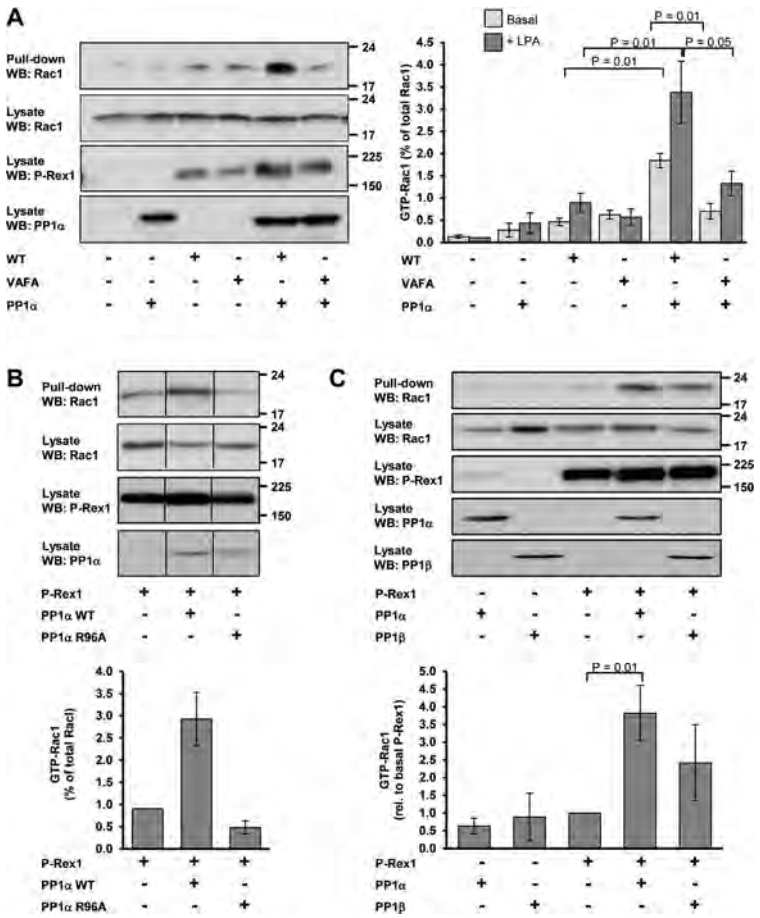

Figure 3 PP1α stimulates P-Rex1 Rac-GEF activity *in vivo*

(**A**) PP1α stimulates P-Rex1 WT, but not P-Rex1 VAFA, Rac-GEF activity *in vivo*. Pak-CRIB pull-down assay for endogenous Rac1 activity in serum-starved HEK-293 cells expressing Myc–P-Rex1 WT, Myc–P-Rex1 VAFA and/or eGFP–PP1α, stimulated with (right-hand panel, dark grey bars) or without (right-hand panel, light grey bars) 50 nM LPA for 1 min. The GTP-loading of Rac1 (left-hand panel, Rac1 activity), and the expression of Rac1 (2 % of the total loaded), P-Rex1 and PP1α were assessed by immunoblotting. The left-hand panel shows blots from one experiment that is representative of four. The right-hand panel shows densitometric analysis of four experiments (two for untransfected cells). Results are means $\pm$ range or S.E.M., as appropriate. Significance was determined using Tukey's Honestly Significant Difference test. (**B**) Phosphatase-dead PP1α cannot stimulate P-Rex1 Rac-GEF activity *in vivo*. Pak-CRIB pull-down assays as in (**A**), measuring P-Rex1 Rac-GEF activity in serum-starved HEK-293 cells upon co-expression with either eGFP–PP1α WT or phosphatase-dead eGFP–PP1α R96A. (**C**) PP1α and PP1β can both stimulate P-Rex1 Rac-GEF activity *in vivo*. Pak-CRIB pull-down assays, as in (**A**), measuring P-Rex1 Rac-GEF activity in serum-starved HEK-293 cells upon co-expression with either eGFP–PP1α or eGFP–PP1β. The left-hand panel shows blots from one experiment that is representative of four. The right-hand panel shows densitometric analysis of four experiments normalized to P-Rex1-only samples. Results are means $\pm$ S.E.M. Significance was determined using a Tukey's Honestly Significant Difference test. In the panels showing blots, the molecular mass is given in kDa on the right-hand side. WB, Western blot.

change) also contributes to P-Rex1 activation by PP1α, notably in the presence of G$\beta\gamma$ subunits (Figure 2D).

PP1α activates P-Rex1 *in vivo*

To test whether PP1α stimulates P-Rex1 GEF activity *in vivo*, we used HEK-293 cells, because of their low basal and high P-Rex1-dependent endogenous Rac1 activity (i.e. GTP-loading of Rac1) [25]. Expression of either Myc–P-Rex1 WT or the PP1α binding-deficient mutant Myc–P-Rex1 VAFA in serum-starved cells induced a 3.5- and 4.7-fold increase in active Rac1 respectively, compared with the untransfected controls (Figure 3A). Expression of PP1α alone also induced a slight (2.3-fold) increase in active Rac1. Importantly though, co-expression of P-Rex1 WT with PP1α resulted in a synergistic 14-fold (i.e. 2.4-fold over additive) increase in active Rac1, demonstrating that PP1α substantially stimulates P-Rex1 Rac-GEF activity *in vivo*. In contrast, co-expression of P-Rex1 VAFA with PP1α induced no such increase. Thus PP1α substantially activates P-Rex1 Rac-GEF activity in mammalian cells in an RVxF motif-dependent manner (Figure 3A).

To investigate whether PP1α stimulation of P-Rex1 Rac-GEF activity is relevant in GPCR signalling, we stimulated HEK-293 cells for 1 min with 50 nM LPA prior to cell lysis. LPA stimulation causes G$\beta\gamma$-subunit release, thereby stimulating P-Rex1 Rac-GEF activity [25]. Whereas LPA stimulation had no effect on Rac1 activity in cells expressing PP1α alone or co-expressing PP1α with P-Rex1 VAFA, it induced a 2-fold increase in Rac1 activity in cells expressing either P Rex1 WT alone or P Rex1 WT together with PP1α (Figure 3A). Therefore PP1α can stimulate the Rac-GEF activity of P-Rex1 *in vivo* either independently of, or in addition to, stimulation by GPCR signalling.

We noted that co-expression with PP1α affected P-Rex1 protein levels in some experiments. To test for a possible correlation with Rac1 activity, we titrated P-Rex1 to induce up to five-fold variation in overexpression levels (Supplementary Figure 2A at http://www.BiochemJ.org/bj/443/bj4430173add.htm). In serum-starved control cells, $\sim$0.3 % of cellular Rac was active (range of

0–0.7 % between experiments), and in P-Rex1-overexpressing cells ∼1 % (range of 0.3–2.5 %), but there was no direct correlation between specific levels of P-Rex1 overexpression and Rac1 activity (Supplementary Figure 2A). Therefore the stimulation of P-Rex1 Rac-GEF activity by PP1α is unlikely to have been affected by the observed fluctuations in P-Rex1 expression levels.

To test whether P-Rex1 activation by PP1α requires phosphatase activity *in vivo*, we used a phosphatase-dead mutant (R96A). PP1α R96A expressed poorly, but under conditions of comparable PP1α WT and PP1α R96A expression levels, PP1α R96A did not stimulate P-Rex1-dependent Rac1 activity, whereas PP1α WT induced the expected robust increase (Figure 3B). Thus, as suggested by the *in vitro* assays, stimulation of P-Rex1 Rac-GEF activity by PP1α is largely dependent upon PP1α phosphatase activity rather than mere protein complex formation.

To investigate whether down-regulation of endogenous PP1α could be sufficient to reduce the Rac-GEF activity of over-expressed P-Rex1, we treated HEK-293 cells with siRNA against PP1α. Under conditions where endogenous PP1α levels were reduced by 90 %, P-Rex1 activity was unaffected (Supplementary Figure S2B). Hence either endogenous PP1α has little effect on P-Rex1 activity in basal cells (but see below), or the reduction of PP1α levels was not sufficient to produce an effect, or there was redundancy with another phosphatase.

Many PP1-interacting proteins can bind PP1α as well as its close homologue PP1β [42]. To assess whether the activation of P-Rex1 shows any PP1 isoform specificity, we expressed P-Rex1 WT together with either PP1α or PP1β in HEK-293 cells and measured endogenous Rac1 activity. Like PP1α, PP1β was also able to stimulate P-Rex1 activity. However, whereas PP1α-dependent stimulation was 3.5-fold, as expected, PP1β-dependent stimulation was merely 2-fold, despite PP1α and PP1β expression levels being similar (Figure 3C). This indicates some degree of isoform specificity in PP1-dependent activation of P-Rex1, with a preference for PP1α.

PP1α stimulates P-Rex1-dependent changes in cell morphology

We next investigated whether PP1α stimulation of P-Rex1 Rac-GEF activity is sufficient to affect cell shape, a major cellular function of Rac. We used PAE cells, for which Rac-dependent morphology is well characterized [36,43]. Serum-starved PAE cells have a kite-shaped morphology with actin stress fibres (Figure 4A). PDGF stimulation of PAE cells causes Rac-dependent lamellipodia formation and membrane ruffling, and increases P-Rex1 activity in a PI3K/PIP_3-dependent manner [2]. High Rac-GEF activity or constitutively active V12-Rac induce spreading and actin polymerization around the edge of PAE cells ('highly-active Rac' shape) (Figure 4A).

PAE cells expressing Myc–P-Rex1 WT or Myc–P-Rex1 WT VAFA with or without eGFP–PP1α were serum-starved, then stimulated or not with PDGF, and their morphology analysed by immunofluorescence microscopy both for lamellipodia/membrane ruffles and 'highly-active Rac' shape. Expression of P-Rex1 WT, P-Rex1 VAFA or PP1α alone did not cause significant changes in cell morphology (Figure 4B and Supplementary Figure S2C). In contrast, co-expression of P-Rex1 WT with PP1α caused a 4-fold increase in 'highly-active Rac' morphology from approximately 3 to 14 % of serum-starved cells, and doubled the proportion of cells with lamellipodia and edge ruffles from 14 to 29 % (Figure 4B and Supplementary Figure S2C), whereas co-expression of P-Rex1 VAFA with PP1α did not. PDGF stimulation further increased the proportion of P-Rex1 WT and PP1α-co-expressing cells with 'highly-active Rac' morphology to 25 % and

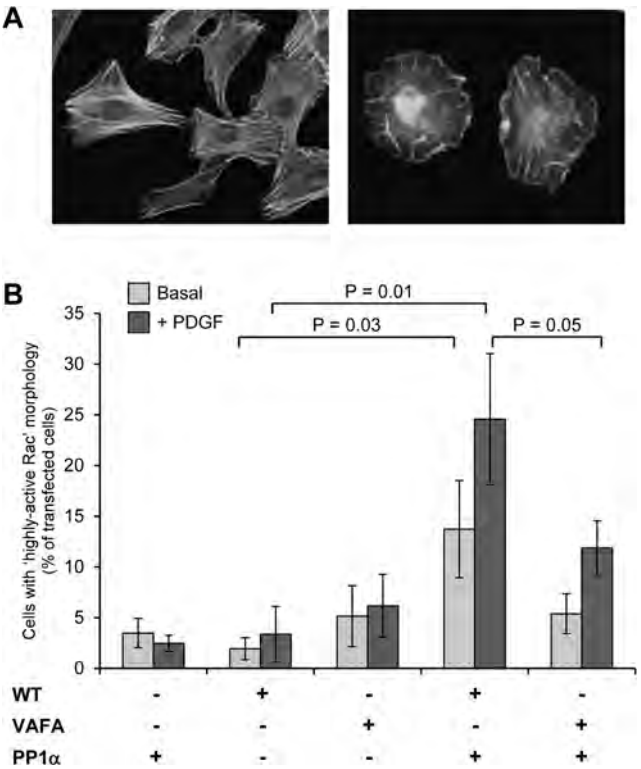

Figure 4 PP1α stimulates P-Rex1-dependent changes in cell morphology in basal and PDGF-stimulated PAE cells

(**A**) Morphology of untransfected (left-hand panel) or V12-Rac-transfected (right-hand panel) PAE cells, revealed by phalloidin staining of the actin cytoskeleton. V12-Rac cells show the characteristic 'highly-active Rac' morphology. (**B**) PP1α stimulates P-Rex1-dependent 'highly-active Rac' morphology in basal (light grey bars) or PDGF-stimulated (dark grey bars) PAE cells. PAE cells overexpressing Myc–P-Rex1 WT or Myc-P-Rex1 VAFA with or without eGFP–PP1α were serum-starved and stimulated for 5 min with 10 ng/ml PDGF (or mock-treated), as indicated, fixed, stained, and P-Rex1 and PP1α expression analysed by immunofluorescence microscopy. In total 100 transfected cells per coverslip, and duplicate coverslips per sample, were scored blind for 'highly-active Rac' morphology as in (**A**). Results are means ± S.E.M. for five independent experiments. Significance was determined using a Student's *t* test.

that of cells with lamellipodia and edge ruffles to 60 % (Figure 4B and Supplementary Figure S2C). Hence PP1α stimulation of P-Rex1 Rac-GEF activity is sufficient to affect Rac-dependent cell responses, both independently of and in addition to receptor-tyrosine kinase/PIP_3-mediated stimulation. This is similar to our findings in HEK-293 cells, where PP1α could act both independently of and in addition to GPCR/Gβγ-mediated stimulation.

PP1α dephosphorylation sites on P-Rex1

As the catalytic activity of PP1α is important for its effects on P-Rex1, we investigated how PP1α affects P-Rex1 phosphorylation. Sf9-cell-derived human EE–P-Rex1 migrates as a doublet on SDS/PAGE which clearly separates on large gels. The upper band is a cytosolic form with relatively low Rac-GEF activity, the lower band is a membrane-bound form with elevated basal activity; P-Rex1 stimulation with PIP_3 and Gβγ causes depletion of the upper and enrichment of the lower band [21,22,25]. When we incubated purified recombinant Sf9-cell-derived EE–P-Rex1 with recombinant PP1α, PP1α caused a reduction in serine phosphorylation particularly of the upper band, suggesting that the inactive cytosolic form of P-Rex1 may be its main target (Figure 5A). Accordingly, immunofluorescence microscopy in

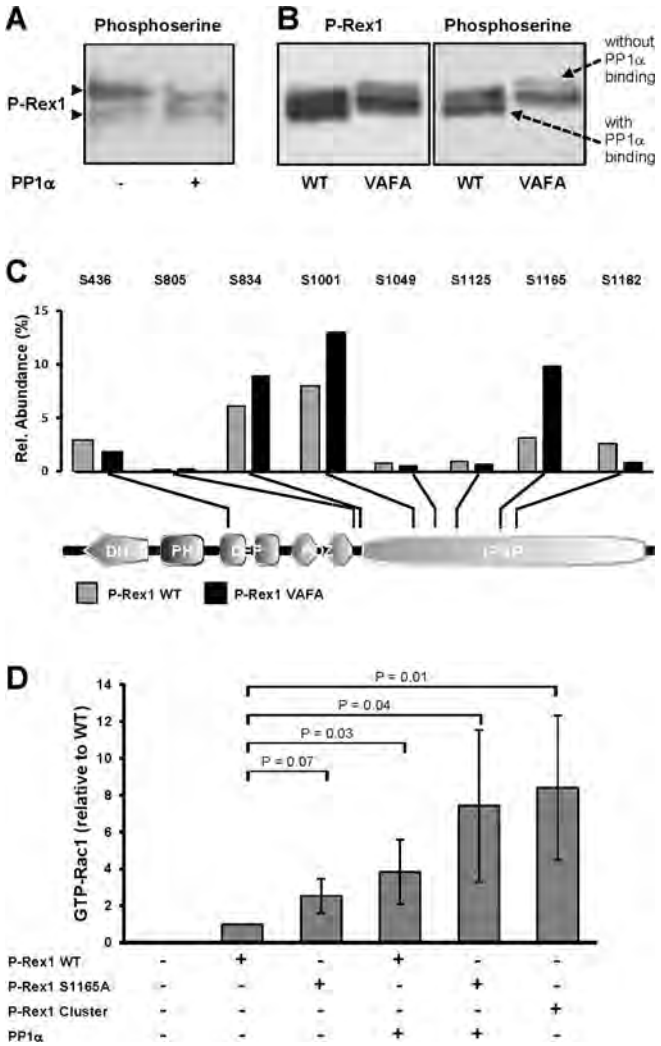

Figure 5 Ser^{1165} is a PP1α target dephosphorylation site on P-Rex1 important in the regulation of P-Rex1 activity

(**A**) Phosphoserine content of purified recombinant Sf9-cell-derived P-Rex1 (25 nM) after incubation with or without recombinant PP1α (500 nM) for 30 min. Shown is a Western blot analysis from one experiment that is representative of two. (**B**) Gel-migration properties of P-Rex1 WT and P-Rex1 VAFA. Lysates of PAE cells expressing EE–P-Rex1 WT or EE–P-Rex1 VAFA together with eGFP–PP1α were subjected to anti-EE immunoprecipitation and precipitates were analysed by anti-P-Rex1 or phosphoserine Western blots as indicated. (**C**) MS of phosphorylation sites in P-Rex1 WT (grey bars) and P-Rex1 VAFA (black bars). EE–P-Rex1 WT and EE–P-Rex1 VAFA were expressed in PAE cells (without exogenous PP1α) and anti–EE immunoprecipitates were subjected to SDS/PAGE. P-Rex1 bands were isolated, digested either with trypsin, chymotrypsin or AspN, and subjected to LC–MS/MS. This achieved 96 % coverage of P-Rex1 and revealed ten phosphopeptides on to which ten serine phosphorylation sites were mapped. Their level of phosphorylation (compared with the total peptide) was measured by MS, and was sufficiently high for analysis in the eight indicated sites. (**D**) P–Rex1 WT, P–Rex1 Ser1165A or P-Rex1 'cluster' mutant were expressed in HEK-293 cells with or without eGFP–PP1α, serum-starved and subjected to a Pak-CRIB pull-down assay to measure endogenous Rac1 activity. Results are means $\pm$ S.E.M. for four independent experiments. Significance was determined using a Student's *t* test.

HEK-293 and PAE cells showed no obvious changes in the largely cytosolic subcellular localizations of P-Rex1 and PP1α upon their co-expression (results not shown).

We next compared the gel-migration properties of EE–P-Rex1 WT and EE–P-Rex1 VAFA upon co-expression with PP1α in basal PAE cells. Immunoprecipitated P-Rex1 WT migrated as a doublet like Sf9-cell-derived P-Rex1, whereas P-Rex1 VAFA lacked the lower band and gained a higher band, indicative of higher phosphorylation levels (Figure 5B). A similar pattern was observed in phosphoserine Western blots (Figure 5B). Hence, although the ability of P-Rex1 to bind PP1α does affect gel migration, it has no major impact on global P-Rex1 phosphoserine levels, suggesting that PP1α target sites represent a minority of all P-Rex1 phosphorylation sites.

To identify the site(s) of PP1α-dependent dephosphorylation, we analysed PAE-cell-derived P-Rex1 WT and P-Rex1 VAFA by MS, reasoning that PP1α target residues would be more highly phosphorylated in P-Rex1 VAFA. Importantly, we did not overexpress PP1α in these experiments, but relied solely on endogenous PP1α in order to reveal only physiologically relevant sites. P-Rex1 WT and P-Rex1 VAFA immunoprecipitates were subjected to SDS/PAGE, and P-Rex1 bands were isolated, digested with three proteases separately (trypsin, chymotrypsin, AspN), and subjected to LC–MS/MS to identify phosphorylated proteolytic fragments. This approach achieved 96 % coverage of P-Rex1 and revealed ten phosphopeptides on to which phosphorylation sites were mapped, resulting in the identification of ten phosphorylated serine residues: Ser^{436}, Ser^{805}, Ser^{834}, Ser^{1001}, Ser^{1049}, Ser^{1125}, Ser^{1165}, Ser^{1182}, Ser^{1191} and Ser^{1200} (Supplementary Figures S3A and S3B at http://www.BiochemJ.org/bj/443/bj4430173add.htm). Tyrosine and threonine phosphorylation was not detected.

The same ten phosphoserine residues were found in P-Rex1 WT and P-Rex1 VAFA, suggesting that either their phosphorylation is PP1α-independent or that endogenous PP1α only dephosphorylates a proportion of P-Rex1 molecules. To test this, we measured the degree of phosphorylation of each peptide by MS. This approach was successful with eight of the ten phosphopeptides (the concentrations of the peptides containing Ser^{1191} and Ser^{1200} were too low for accurate quantification). It showed that the phosphorylation level of each peptide was low, ranging from $\leqslant$1 to 13 % of molecules. Importantly though, phosphorylation of three serine residues, namely Ser^{834}, Ser^{1001} and Ser^{1165}, was stronger in P-Rex1 VAFA than P-Rex1 WT, suggesting that the ability of P-Rex1 to bind PP1α is required for dephosphorylation of these sites (Figure 5C). Thus these three serine residues are candidate sites for PP1α-dependent dephosphorylation. In contrast, the other sites showed no different or higher phosphorylation in P-Rex1 WT than P-Rex1 VAFA and are therefore unlikely to be PP1α targets.

Ser^{1165} is a phosphorylation site important in the regulation of P-Rex1 activity

Of the three candidate residues, Ser^{1165} showed the greatest (3-fold) difference in phosphorylation between P-Rex1 WT and P-Rex1 VAFA (Figure 5C) and was also most evolutionarily conserved (Supplementary Figure S3C). We therefore considered Ser^{1165} likely to be the most important PP1α target site. To test this, we generated a P-Rex1 S1165A point mutant and assayed the effects of the mutation on P-Rex1 Rac-GEF activity in HEK-293 cells. P-Rex1 S1165A had 3-fold higher Rac-GEF activity than P-Rex1 WT, similar to PP1α-stimulated P-Rex1 WT activity (Figure 5D), suggesting that the alanine mutation mimics the dephosphorylated state of Ser^{1165}. Therefore Ser^{1165} seems to be a major PP1α target site in P-Rex1 and is important in the regulation of P-Rex1 activity.

Finally, as predicted from the MS analysis, we found that Ser^{1165} was not the only PP1α target site, because co-expression of P-Rex1 S1165A with PP1α induced even higher Rac1 activity than expression of P-Rex1 S1165A alone (Figure 5D). In an attempt to identify further residues that may contribute to P-Rex1 regulation, we generated a P-Rex1 mutant comprising alanine

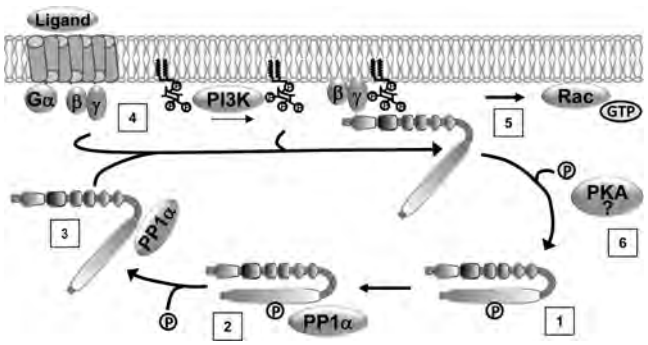

Figure 6 Model of the regulation of P-Rex1 by PP1α

[1] Inactive cytosolic P-Rex1 is phosphorylated on Ser^{1165} and other serine residues and is in a closed conformation. [2] PP1α binds to the RVxF motif in the IP4P domain of P-Rex1 and dephosphorylates Ser^{1165} and probably two or more other serine residues. [3] This releases steric inhibition of the DH/PH domain tandem by the C-terminal domains, inducing higher basal activity and increased accessibility to G$\beta\gamma$ subunits and PIP_3. At some point prior to P-Rex1 membrane translocation, PP1α may dissociate. [4] Stimulation of GPCRs and PI3K-coupled receptors induces G$\beta\gamma$ subunit release and production of PIP_3 respectively. G$\beta\gamma$ subunits and PIP_3 bind P-Rex1, stimulating stable membrane association and further activation of P-Rex1. [5] Active P-Rex1 catalyses guanine-nucleotide exchange on Rac for GTP (activation). [6] Upon cessation of G$\beta\gamma$ and PIP_3 signals, P-Rex1 translocates back to the cytosol and is phosphorylated by PKA [25] and possibly PKB or PKCδ [27]. Phosphorylation by PKA inactivates P-Rex1. It remains to be seen whether PKA is the kinase responsible for phosphorylation of Ser^{1165}.

mutations in Ser^{1165} as well as four neighbouring serine residues. One of these additional residues was Ser^{1182}, identified as a phosphorylation site in the present study and also highly conserved (Figure 5C and Supplementary Figure S3C), and the others (Ser^{1169}, Ser^{1179} and Ser^{1185}) were identified as phosphorylation sites in a separate project (S. Thelen and M. Thelen, unpublished work). Indeed, this P-Rex1 'cluster' mutant showed a similar level of Rac1-GEF activity as P-Rex1 S1165A co-expressed with PP1α (Figure 5D), indicating that among the serine residues neighbouring Ser^{1165} there may be further PP1α target sites.

In summary, we have shown that PP1α directly binds P-Rex1 through an RVxF motif and dephosphorylates and thereby activates P-Rex1 in a physiologically relevant manner on Ser^{1165} and probably other residues. A model of how PP1α regulates P-Rex1 in relation to the known mechanisms of regulation through PIP_3, G$\beta\gamma$ and PKA is shown in Figure 6.

DISCUSSION

We have identified PP1α-dependent dephosphorylation as a novel mechanism of P-Rex1 regulation. PP1α binds P-Rex1 through an 'RVxF' motif and dephosphorylates P-Rex1 on Ser^{1165}, thereby stimulating P-Rex1 Rac-GEF activity. Previous mutagenesis work has suggested that the C-terminal domains of P-Rex1 are autoinhibitory under basal conditions, presumably by folding back on to the catalytic DH/PH tandem [21,22,24]. The results of the present study support a model in which PP1α-dependent dephosphorylation of P-Rex1 Ser^{1165} releases this autoinhibition, thus promoting an open conformation with elevated basal activity. This probably also facilitates binding of G$\beta\gamma$ and PIP_3, as PP1α can activate P-Rex1 both independently of and in addition to G$\beta\gamma$ and PIP_3. The results of the present study also show that regulation by PP1α is not absolutely required for P-Rex1 GEF activity, as the PP1α-binding deficient P-Rex1 VAFA mutant had near-normal basal activity *in vivo*. Hence the role of PP1α seems to be to facilitate P-Rex activation.

P-Rex1 and P-Rex2 both bind PP1α through their RVxF motif. Therefore it is highly probable that P-Rex2 is dephosphorylated and activated by PP1α in the same manner as P-Rex1. The RVxF motif is in the P-Rex IP4P domain, which has homology with phosphatases, but seems devoid of phosphatase activity. It would be interesting to re-iterate the search for activity in the presence of bound phosphatase-dead PP1α, to see whether its binding can unmask a cryptic IP4P phosphatase activity although this seems unlikely given that protein binding usually inhibits phosphatases. Some PP1α-interacting proteins have more sites of contact with PP1α than just the RVxF motif [42]. Two additional PP1α-binding motifs have been identified, 'MyPhoNE' and 'SILK' [31]. However, as mutation of the RVxF motif was sufficient to eliminate P-Rex1 binding to PP1α, and neither of these additional motifs are present in P-Rex1 or P-Rex2, it seems unlikely that important secondary-binding sites exist in P-Rex. Of note, the splice variant P-Rex2b does not contain an RVxF motif (it lacks the entire C-terminal half), suggesting that the mechanisms of regulation differ between this form and the other P-Rex family members.

Activation of P-Rex1 requires the catalytic activity of PP1α, as okadaic acid treatment and phosphatase-dead PP1α have shown. However, at least in the presence of G$\beta\gamma$, inhibition of PP1α only partially blocked P-Rex1 activity. This suggested that PP1α has additional activity-independent effects on P-Rex1, presumably through binding-induced conformational changes. Future structural analysis will be required to address this possibility.

RNAi (RNA interference)-mediated down-regulation of endogenous PP1α had no obvious effect on P-Rex1 activity, although MS confirmed that endogenous PP1α does dephosphorylate P-Rex1. Hence the 90 % PP1α knockdown achieved in HEK-293 cells was either insufficient to affect P-Rex1 activity or it revealed a redundancy with PP1β, which is also able to stimulate P-Rex1 activity, albeit less well. The three isoforms of PP1 (PP1α, -β and -γ) are 90 % identical and all bind the RVxF motif, so binding partners commonly interact with more than one isoform. Hence although it was surprising to find even partial isoform preference, PP1β probably plays a somewhat redundant role to PP1α in P-Rex1 regulation.

It would be of interest to determine the subcellular localizations of P-Rex1 VAFA and P-Rex1 S1165A. Our model predicts that dephosphorylation of Ser^{1165} facilitates binding of G$\beta\gamma$ and PIP_3, and therefore potentially also membrane association. However, our imaging experiments to date have not revealed an obvious influence of P-Rex1 WT/PP1α co-expression on the subcellular localization of either protein, so effects on localization are likely to be subtle at best.

It remains to be seen if the interaction between P-Rex1 and PP1α is regulated by signalling events. *In vitro* activation of P-Rex1 by PP1α does not require additional proteins, but it seems likely that, in the cell, other binding partners mediate signalling inputs to provide temporal and spatial control. Furthermore, endogenous PP1α has relatively minor effects on global P-Rex1 phosphorylation levels. It is possible that the inhibition of PP1α by P-Rex1 observed *in vitro* also applies *in vivo*, thus limiting the extent of P-Rex1 dephosphorylation. PP1α might dephosphorylate P-Rex1 upon first contact, before being inhibited, and this inhibition might also be sensitive to control by further binding partners.

The regulation of P-Rex1 GEF activity through phosphorylation is far more complex than previously appreciated. We have identified three candidate PP1α target serine residues, and followed up Ser^{1165} as it showed the biggest difference in phosphorylation between P-Rex1 WT and P-Rex1 VAFA, and is perfectly conserved. Indeed, loss of Ser^{1165} phosphorylation (S1165A mutant) resulted in a 3-fold increase in basal P-Rex1 Rac-GEF activity. However, correlation of Ser^{1165} phosphorylation levels with

in vivo Rac-GEF activity levels is not straightforward and should be addressed *in vitro* in the future by assessing the Rac-GEF activities of purified recombinant P-Rex1 proteins with the relevant phospho-deficient and phospho-mimetic point mutations. Future analysis of Ser^{834} and Ser^{1001}, as well as individual serine residues in the P-Rex1 cluster mutant, is likely to reveal further PP1α-dependent sites. Of the seven other phosphoserine residue sites identified, two more (Ser^{1191} and Ser^{1200}) may be PP1α targets, but their phosphorylation levels were too low for further analysis. The five remaining sites (Ser^{436}, Ser^{805}, Ser^{1049}, Ser^{1125} and Ser^{1182}) are likely to be PP1α-independent, as they were equally or more highly phosphorylated in P-Rex1 WT than P-Rex1 VAFA. Of these, Ser^{436} was previously described as constitutively phosphorylated in HL60 cells [44]. We also identified more phosphoserine residues in a separate project (the P-Rex1 cluster mutant; S. Thelen and M. Thelen, unpublished work), and four further sites have recently been described which are affected by receptor tyrosine kinase signalling in breast cancer cells [17]. All these sites must be under the direct control of serine kinases and phosphatases, and are potentially capable of regulating P-Rex1 activity, protein complex formation and/or subcellular localization.

Inhibition of P-Rex1 GEF activity by PKA-mediated phosphorylation has been described previously [25]. It remains to be seen if PKA is the kinase that reverses the activation of P-Rex1 by PP1α. The simplest model would include PP1α-mediated dephosphorylation and activation, followed by PKA phosphorylating the same residue to switch-off activity. Such a simple mechanism appears unlikely, as Ser^{1165} does not lie within a PKA consensus sequence and PP1α is not absolutely required for P-Rex1 activity, whereas PKA phosphorylation abrogates P-Rex1 stimulation by G$\beta\gamma$ and PIP_3. Therefore PKA is unlikely to be the kinase that reverses the effects of PP1α. This implies the existence of further activating serine phosphatases in P-Rex1 regulation. Interestingly, PKCδ and PKB have recently been shown to stimulate P-Rex1-dependent ROS production in COS^{phox} cells [27]. Future studies will show whether P-Rex1 is a direct target of PKB or PKCδ. In any event, it is already clear that P-Rex1 regulation is a complex integration of many kinase and phosphatase activities, which tie P-Rex1 into a much wider signalling network than previously appreciated.

There are a limited number of other examples of serine/threonine phosphatase involvement in GEF regulation. The Arf GEFs BIG (brefeldin A-inhibited guanine-nucleotide-exchange protein) 1 and BIG2 interact with PP1γ *in vivo* and are stimulated by PP1γ *in vitro* [45]; the Arf-GEF BIG3 and the putative Rho-GEF FARP1 [FERM, RhoGEF (ARHGEF) and pleckstrin domain protein 1 (chondrocyte-derived)] are likely interactors of PP1α [31], and the Rap-GEF C3G (Rap GEF1) targets PP2A (protein phosphatase 2A) to the actin cytoskeleton, enabling dephosphorylation of ERK (extracellular-signal-regulated kinase) and suppression of malignant transformation [46]. Finally, although phosphorylation is probably the most common mechanism of regulation in Rho-GEFs, and the kinases involved have often been studied in great detail, the present study is to our knowledge the first to characterize the Rho-GEF regulation by a serine/threonine phosphatase. It will be exciting to determine the impact of this new mechanism of regulation on the functional roles of P-Rex family GEFs in neuronal disorders, inflammation and cancer biology.

AUTHOR CONTRIBUTION

Mark Barber and Heidi Welch designed and performed the experiments and wrote the paper; Annick Hendrickx and Sylvia Thelens performed experimental work; Hugo Ceulemans performed the bioinformatics analysis; David Oxley performed the MS and analysis; and Marcus Thelen and Mathieu Bollen designed experiments.

ACKNOWLEDGEMENTS

The PP1α R96A mutant was a gift from Professor Angus Nairn (Department of Psychiatry, Yale University, New Haven, CT, U.S.A.). P-Rex1 VAFA was generated with the kind help of Dr Yanfeng Dai. We thank Dr Judith Webster from the Babraham Mass Spectrometry Facility.

FUNDING

This work was supported through Biotechnology and Biological Sciences Research Council (BBSRC) [grant number 521-120-C233] core support to the Mass Spectrometry Facility and the Cambridge Commonwealth Trust (Ph.D. studentship to M.A.B).

REFERENCES

1 Wennerberg, K., Rossman, K. L. and Der, C. J. (2005) The Ras superfamily at a glance. J. Cell Sci. **118**, 843–846
2 Welch, H. C., Coadwell, W. J., Ellson, C. D., Ferguson, G. J., Andrews, S. R., Erdjument-Bromage, H., Tempst, P., Hawkins, P. T. and Stephens, L. R. (2002) P-Rex1, a PtdIns(3,4,5)*P*3- and G$\beta\gamma$-regulated guanine-nucleotide exchange factor for Rac. Cell **108**, 809–821
3 Donald, S., Hill, K., Lecureuil, C., Barnouin, R., Krugmann, S., Coadwell, W. J., Andrews, S. R., Walker, S. A., Hawkins, P. T., Stephens, L. R. and Welch, H. C. (2004) P-Rex2, a new guanine-nucleotide exchange factor for Rac. FEBS Lett. **572**, 172–176
4 Rosenfeldt, H., Vazquez-Prado, J. and Gutkind, J. S. (2004) P-Rex2, a novel PI-3-kinase sensitive Rac exchange factor. FEBS Lett. **572**, 167–171
5 Donald, S., Humby, T., Fyfe, I., Segonds-Pichon, A., Walker, S. A., Andrews, S. R., Coadwell, W. J., Emson, P., Wilkinson, L. S. and Welch, H.C.E. (2008) P-Rex2 regulates Purkinje cell dendrite morphology and motor coordination. Proc. Natl. Acad. Sci. U.S.A. **105**, 4483–4488
6 Yoshizawa, M., Kawauchi, T., Sone, M., Nishimura, Y. V., Terao, M., Chihama, K., Nabeshima, Y. and Hoshino, M. (2005) Involvement of a Rac activator, P-Rex1, in neurotrophin-derived signaling and neuronal migration. J. Neurosci. **25**, 4406–4419
7 Li, Z., Paik, J. H., Wang, Z., Hla, T. and Wu, D. (2005) Role of guanine nucleotide exchange factor P-Rex2b in sphingosine 1-phosphate-induced Rac1 activation and cell migration in endothelial cells. Prostaglandins Other Lipid Mediators **76**, 95–104
8 Dong, X., Mo, Z., Bokoch, G., Guo, C., Li, Z. and Wu, D. (2005) P-Rex1 is a primary Rac2 guanine nucleotide exchange factor in mouse neutrophils. Curr. Biol. **15**, 1874–1879
9 Wang, Z., Dong, X., Li, Z., Smith, J. D. and Wu, D. (2008) Lack of a significant role of P-Rex1, a major regulator of macrophage Rac1 activation and chemotaxis, in atherogenesis. Prostaglandins Other Lipid Mediators **87**, 9–13
10 Welch, H. C., Condliffe, A. M., Milne, L. J., Ferguson, G. J., Hill, K., Webb, L. M., Okkenhaug, K., Coadwell, W. J., Andrews, S. R., Thelen, M. et al. (2005) P-Rex1 regulates neutrophil function. Curr. Biol. **15**, 1867–1873
11 Waters, J. E., Astle, M. V., Ooms, L. M., Balamatsias, D., Gurung, R. and Mitchell, C. A. (2008) P-Rex1: a multidomain protein that regulates neurite differentiation. J. Cell Sci. **121**, 2892–2903
12 Lawson, C., Donald, S., Anderson, K., Patton, D. and Welch, H. (2011) P-Rex1 and Vav1 cooperate in the regulation of fMLF-dependent neutrophil responses. J. Immunol. **186**, 1467–1476
13 Ledezma-Sánchez, B. A., García-Regalado, A., Guzmán-Hernández, M. L. and Vázquez-Prado, J. (2010) Sphingosine-1-phosphate receptor S1P1 is regulated by direct interactions with P-Rex1, a Rac guanine nucleotide exchange factor. Biochem. Biophys. Res. Commun. **391**, 1647–1652
14 Carretero-Ortega, J., Walsh, C. T., Hernández-García, R., Reyes-Cruz, G., Brown, J. H. and Vázquez-Prado, J. (2010) Phosphatidylinositol 3,4,5-triphosphate-dependent Rac exchanger 1 (P-Rex-1), a guanine nucleotide exchange factor for Rac, mediates angiogenic responses to stromal cell-derived factor-1/chemokine stromal cell derived factor-1 (SDF-1/CXCL-12) linked to Rac activation, endothelial cell migration, and *in vitro* angiogenesis. Mol. Pharmacol. **77**, 435–442
15 Jackson, C., Welch, H. C. and Bellamy, T. C. (2010) Control of cerebellar long-term potentiation by P-Rex-family guanine-nucleotide exchange factors and phosphoinositide 3-kinase. PLoS ONE **5**, e11962
16 Lindsay, C. R., Lawn, S., Campbell, A. D., Faller, W. J., Rambow, F., Mort, R. L., Timpson, P., Li, A., Cammareri, P., Ridgway, R. A. et al. (2011) P-Rex1 is required for efficient melanoblast migration and melanoma metastasis. Nat. Commun. **2**, 555

17 Montero, J. C., Seoane, S., Ocana, A. and Pandiella, A. (2010) P-Rex1 participates in Neuregulin-ErbB signal transduction and its expression correlates with patient outcome in breast cancer. Oncogene **30**, 1059–1071

18 Qin, J., Xie, Y., Wang, B., Hoshino, M., Wolff, D. W., Zhao, J., Scofield, M. A., Dowd, F. J., Lin, M. F. and Tu, Y. (2009) Upregulation of PIP3-dependent Rac exchanger 1 (P-Rex1) promotes prostate cancer metastasis. Oncogene **28**, 1853–1863

19 Sosa, M. S., Lopez-Haber, C., Yang, C., Wang, H., Lemmon, M. A., Busillo, J. M., Luo, J., Benovic, J. L., Klein-Szanto, A., Yagi, H. et al. (2010) Identification of the Rac-GEF P-Rex1 as an essential mediator of ErbB signaling in breast cancer. Mol. Cell **40**, 877–892

20 Fine, B., Hodakoski, C., Koujak, S., Su, T., Saal, L. H., Maurer, M., Hopkins, B., Keniry, M., Sulis, M. L., Mense, S. et al. (2009) Activation of the PI3K pathway in cancer through inhibition of PTEN by exchange factor P-Rex2a. Science **325**, 1261–1265

21 Hill, K., Krugmann, S., Andrews, S. R., Coadwell, W. J., Finan, P., Welch, H. C., Hawkins, P. T. and Stephens, L. R. (2005) Regulation of P-Rex1 by phosphatidylinositol (3,4,5)-trisphosphate and G$\beta\gamma$ subunits. J. Biol. Chem. **280**, 4166–4173

22 Barber, M. A., Donald, S., Thelen, S., Anderson, K. E., Thelen, M. and Welch, H.C.E. (2007) Membrane translocation of P-Rex1 is mediated by G protein $\beta\gamma$ subunits and phosphoinositide 3-kinase. J. Biol. Chem. **282**, 29967–29976

23 Mayeenuddin, L. H., McIntire, W. E. and Garrison, J. C. (2006) Differential sensitivity of P-Rex1 to isoforms of G protein $\beta\gamma$ dimers. J. Biol. Chem. **281**, 1913–1920

24 Urano, D., Nakata, A., Mizuno, N., Tago, K. and Itoh, H. (2008) Domain–domain interaction of P-Rex1 is essential for the activation and inhibition by G protein $\beta\gamma$ subunits and PKA. Cell. Signaling **20**, 1545–1554

25 Mayeenuddin, L. H. and Garrison, J. C. (2006) Phosphorylation of P-Rex1 by the cyclic AMP-dependent protein kinase inhibits the phosphatidylinositiol (3,4,5)-trisphosphate and G$\beta\gamma$-mediated regulation of its activity. J. Biol. Chem. **281**, 1921–1928

26 Zhao, T., Nalbant, P., Hoshino, M., Dong, X., Wu, D. and Bokoch, G. M. (2007) Signaling requirements for translocation of P-Rex1, a key Rac2 exchange factor involved in chemoattractant-stimulated human neutrophil function. J. Leukocyte Biol. **81**, 1127–1136

27 Nie, B., Cheng, N., Dinauer, M. C. and Ye, R. D. (2010) Characterization of P-Rex1 for its role in fMet-Leu-Phe-induced superoxide production in reconstituted COS^{phox} cells. Cell. Signalling **22**, 770–782

28 Bollen, M., Peti, W., Ragusa, M. J. and Beullens, M. (2010) The extended PP1 toolkit: designed to create specificity. Trends Biochem. Sci. **35**, 450–458

29 Virshup, D. M. and Shenolikar, S. (2009) From promiscuity to precision: protein phosphatases get a makeover. Mol. Cell **33**, 537–545

30 Wakula, P., Beullens, M., Ceulemans, H., Stalmans, W. and Bollen, M. (2003) Degeneracy and function of the ubiquitous RVXF motif that mediates binding to protein phosphatase-1. J. Biol. Chem. **278**, 18817–18823

31 Hendrickx, A., Beullens, M., Ceulemans, H., Den Abt, T., Van Eynde, A., Nicolaescu, E., Lesage, B. and Bollen, M. (2009) Docking motif-guided mapping of the interactome of protein phosphatase-1. Chem. Biol. **16**, 365–371

32 Roy, J. and Cyert, M. S. (2009) Cracking the phosphatase code: docking interactions determine substrate specificity. Sci. Signaling **2**, re9

33 Beullens, M., Vulsteke, V., Van Eynde, A., Jagiello, I., Stalmans, W. and Bollen, M. (2000) The C-terminus of NIPP1 (nuclear inhibitor of protein phosphatase-1) contains a novel binding site for protein phosphatase-1 that is controlled by tyrosine phosphorylation and RNA binding. Biochem. J. **352**, 651–658

34 Hill, K. and Welch, H. C. (2006) Purification of P-Rex1 from neutrophils and nucleotide exchange assay. Methods Enzymol. **406**, 26–41

35 DeGuzman, A. and Lee, E. Y. (1988) Preparation of low-molecular-weight forms of rabbit muscle protein phosphatase. Methods Enzymol. **159**, 356–368

36 Welch, H., Eguinoa, A., Stephens, L. R. and Hawkins, P. T. (1998) Protein kinase B and Rac are activated in parallel within a phosphatidylinositide 3OH-kinase-controlled signaling pathway. J. Biol. Chem. **273**, 11248–11256

37 Wakula, P., Beullens, M., van Eynde, A., Ceulemans, H., Stalmans, W. and Bollen, M. (2006) The translation initation factor eIF2β is an interactor of protein phosphatase-1. Biochem. J. **400**, 377–383

38 Sander, E. E., van Delft, S., ten Klooster, J. P., Reid, T., van der Kammen, R. A., Michiels, F. and Collard, J. G. (1998) Matrix-dependent Tiam1/Rac signaling in epithelial cells promotes either cell–cell adhesion or cell migration and is regulated by phosphatidylinositol 3-kinase. J. Cell Biol. **143**, 1385–1398

39 Lesage, B., Beullens, M., Nuytten, M., Van Eynde, A., Keppens, S., Himpens, B. and Bollen, M. (2004) Interactor-mediated nuclear translocation and retention of protein phosphatase-1. J. Biol. Chem. **279**, 55978–55984

40 Dawson, J. and Holmes, C. (1999) Molecular mechanisms underlying inhibition of protein phosphatases my marine toxins. Front. Biosci. **1**, 646–658

41 Haystead, T.A.J., Sim, A.T.R., Carling, D., Honnor, R. C., Tsukitani, Y., Cohen, P. and Hardie, D. G. (1989) Effects of the tumour promoter okadaic acid on intracellular protein phosphorylation and metabolism. Nature **337**, 78–81

42 Ceulemans, H. and Bollen, M. (2004) Functional diversity of protein phosphatase-1, a cellular economizer and reset button. Physiol. Rev. **84**, 1–39

43 Hawkins, P. T., Eguinoa, A., Qiu, R.-G., Stokoe, D., Cooke, F. T., Walters, R., Wennström, S., Claesson-Welsh, L., Evans, T., Symons, M. and Stephens, L. (1995) PDGF stimulates an increase in GTP-Rac via activation of phosphoinositide 3-kinase. Curr. Biol. **5**, 393–403

44 Imami, K., Sugiyama, N., Kyono, Y., Tomita, M. and Ishihama, Y. (2008) Automated phosphoproteome analysis for cultured cancer cells by two-dimensional nanoLC–MS using a calcined titania/C18 biphasic column. Anal. Sci. **24**, 161–166

45 Kuroda, F., Moss, J. and Vaughan, M. (2007) Regulation of brefeldin A-inhibited guanine nucleotide-exchange protein 1 (BIG1) and BIG2 activity via PKA and protein phosphatase 1γ. Proc. Natl. Acad. Sci. U.S.A. **104**, 3201–3206

46 Martín-Encabo, S., Santos, E. and Guerrero, C. (2007) C3G mediated suppression of malignant transformation involves activation of PP2A phosphatases at the subcortical actin cytoskeleton. Exp. Cell Res. **313**, 3881–3891

Received 28 November 2011/10 January 2012; accepted 16 January 2012
Published as BJ Immediate Publication 16 January 2012, doi:10.1042/BJ20112078

Biochem. J. (2012) **443**, 173–183 (Printed in Great Britain) doi:10.1042/BJ20112078

online data

SUPPLEMENTARY ONLINE DATA

The guanine-nucleotide-exchange factor P-Rex1 is activated by protein phosphatase 1α

Mark A. BARBER*, Annick HENDRICKX†, Monique BEULLENS†, Hugo CEULEMANS†, David OXLEY‡, Sylvia THELEN§, Marcus THELEN§, Mathieu BOLLEN† and Heidi C. E. WELCH*[1]

*Inositide Programme, Babraham Institute, Cambridge, U.K., †Department of Molecular Cell Biology, Catholic University Leuven, Leuven, Belgium, ‡Proteomics Group, Babraham Institute, Cambridge, U.K., and §Institute for Research in Biomedicine, Bellinzona, Switzerland

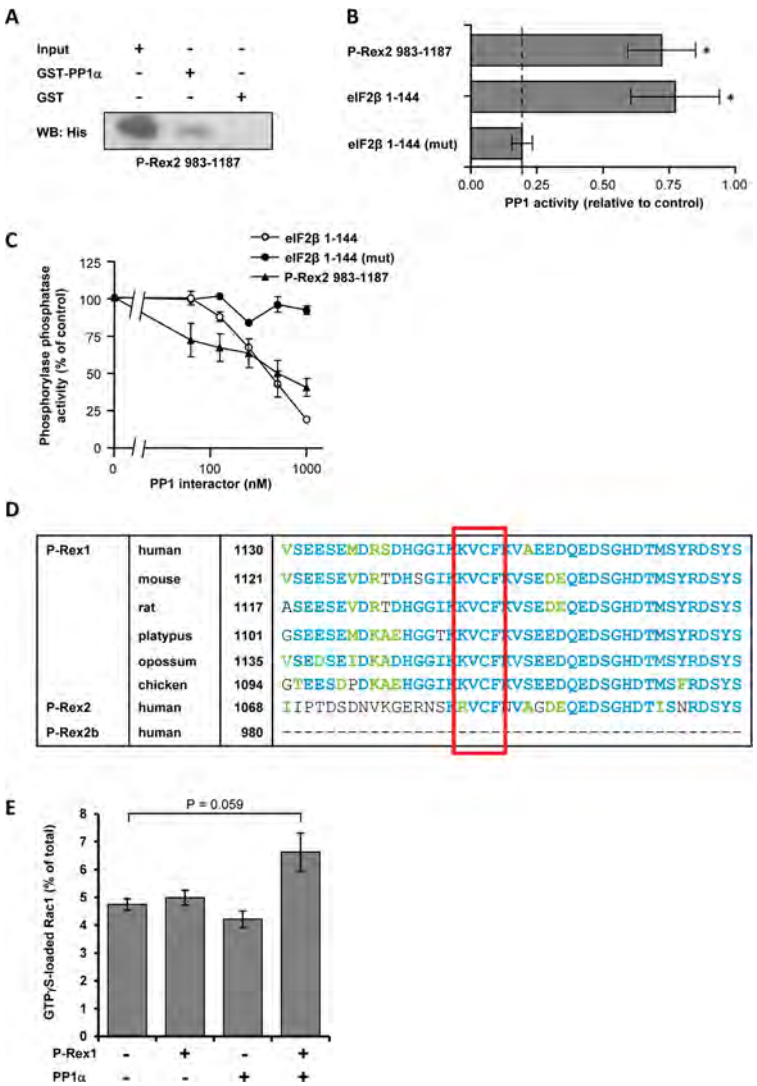

Figure S1 P-Rex2 is a PP1α-binding protein

(**A**) Bacterially expressed purified His-tagged P-Rex2 fragment 983–1187 was incubated with purified GST–PP1α or GST immobilized on glutathione agarose and binding revealed by immunoblotting with anti-His antibody. WB, Western blot. (**B**) His–P-Rex2-(983–1187) was immobilized on Ni^{2+}-Sepharose, incubated with purified native rabbit PP1 and binding assessed by trypsin-revealed phosphorylase phosphatase assay using eIF2β-(1–144) as a positive and eIF2β-(1 – 144) (mut) with a mutated RVxF motif as a negative control. Results are means $\pm$ S.E.M. [$n = 3$, $^*P < 0.05$ compared with eIF2β-(1–144) determined by a paired Student's t test]. (**C**) Dose-dependent inhibition of the phosphorylase phosphatase activity of purified rabbit PP1 by purified His–P-Rex2-(983–1187) in comparison with eIF2β-(1–144) and eIF2β-(1–144) (mut). Results are means $\pm$ S.E.M. ($n = 3$). (**D**) P-Rex1 amino acid sequences for all vertebrate species represented in GenBank® were aligned with human P-Rex2 and P-Rex2b using ClustalX and analysed for the presence of an RVxF-type PP1-binding motif (red box). P-Rex2b terminates before the RVxF motif. Blue, conserved residues; green, functionally similar residues; black, divergent residues. Significance was determined by a Student's t test. (**E**) Recombinant PP1α stimulates basal P-Rex1 Rac1-GEF activity *in vitro*. Basal P-Rex1 Rac-GEF activity was assayed as in Figure 2(B) of the main text, except that purified Sf9-cell-derived human full-length EE–Rac1 was used as a substrate instead of EE–Rac2. Results are means $\pm$ range; significance was determined by a Student's t test.

[1] To whom correspondence should be addressed (email heidi.welch@babraham.ac.uk).

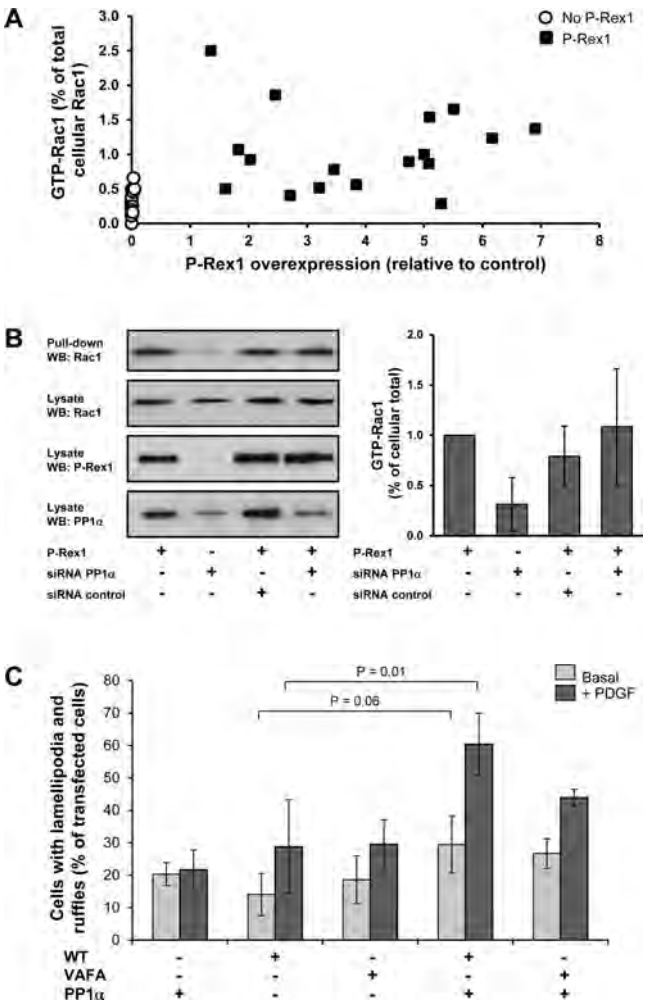

Figure S2 Effects of P-Rex1 and PP1α expression levels on endogenous Rac1 activity

(**A**) Endogenous Rac1 activity is not significantly affected by 5-fold variations in P-Rex1 overexpression levels. Myc–P-Rex1 WT levels were titrated over an approximately 5-fold range by varying the amount of plasmid used for transfection of HEK-293 cells. Cells were serum-starved and subjected to a Pak-CRIB assay. Endogenous Rac1 activity (GTP loading) is plotted against P-Rex1 overexpression levels (■; compared with standard P-Rex1 overexpression) and endogenous P-Rex1 levels (○). Data are pooled from nine experiments. (**B**) siRNA-mediated down-regulation of endogenous PP1α levels does not affect basal P-Rex1 Rac-GEF activity. Myc–P-Rex1 was overexpressed in HEK-293 cells concomitantly with siRNA-mediated knockdown of PP1α expression or mock knockdown with control siRNA. Cells were serum-starved and subjected to a Pak-CRIB assay to measure endogenous Rac1 activity. Left-hand panel: Western blots from one experiment that is representative of three. Right-hand panel: densitometric analysis. Results are means ± S.E.M. for three experiments. (**C**) PP1α stimulates P-Rex1-dependent lamellipodia formation and membrane ruffling in basal (light grey bars) or PDGF-stimulated (dark grey bars) PAE cells. PAE cells overexpressing Myc–P-Rex1 WT or Myc–P-Rex1 VAFA with or without eGFP–PP1α were serum-starved and stimulated for 5 min with 10 ng/ml PDGF (or mock treated), as indicated, fixed, stained, and P-Rex1 and PP1α expression analysed by immunofluorescence microscopy. For each coverslip 100 transfected cells, and duplicate coverslips per sample, were scored blind for 'highly-active Rac' morphology as in (**A**). Results are means ± S.E.M. for five independent experiments. Significance was determined by a Student's *t* test.

A

Site	Peptide
S436	KL**S**TVPK
S805	EARASQEA**S**TE
S834	SLGPRL**S**LCEDSPMoxVTL
S1001	GRKP**S**LIGLDPEQGHLNPMoxSY
S1049	DG**S**FGPASGTLGQE
S1125	EEAS**S**LPLVSEESEMox
S1165	DTMox**S**YR
S1182	DSVL**S**YTSVR
S1191	SNS**S**YLGSDEMoxGSGDELPCDMoxR
S1200	LGSDEMoxG**S**GDELPCDMoxR

B

```
   1 MEAPSGSEPG GDGAGDCAHP DPRAPGAAAP SSGPGPCAAA RESERQLRLR LCVLNEILGT
  61 ERDYVGTLRF LQSAFLHRIR QNVADSVEKG LTEENVKVLF SNIEDILEVH KDFLAALEYC
 121 LHPEPQSQHE LGNVFLKFKD KFCVYEEYCS NHEKALRLLV ELNKIPTVRA FLLSCMLLGG
 181 RKTTDIPLEG YLLSPIQRIC KYPLLLKELA KRTPGKHPDH PAVQSALQAM KTVCSNINET
 241 KRQMEKLEAL EQLQSHIEGW EGSNLTDICT QLLLQGTLLK ISAGNIQERA FFLFDNLLVY
 301 CKRKSRVTGS KKSTKRTKSI NGSLYIFRGR INTEVMEVEN VEDGTADYHS NGYTVTNGWK
 361 IHNTAKNKWF VCMAKTAEEK QKWLDAIIRE REQRESLKLG MERDAYVMIA EKGEKLYHMM
 421 MNKKVNLIKD RRRKLSTVPK CFLGNEFVAW LLEIGEISKT EEGVNLGQAL LENGIIHHVS
 481 DKHQFKNEQV MYRFRYDDGT YKARSELEDI MSKGVRLYCR LHSLYTPVIK DRDYHLKTYK
 541 SVLPGSKLVD WLLAQGDCQT REEAVALGVG LCNNGFMHHV LEKSEFRDES QYFRFHADEE
 601 MEGTSSKNKQ LRNDFKLVEN ILAKRLLILP QEEDYGFDIE EKNKAVVVKS VQRGSLAEVA
 661 GLQVGRKIYS INEDLVFLRP FSEVESILNQ SFCSRRPLRL LVATKAKEII KIPDQPDTLC
 721 FQIRGAAPPY VYAVGRGSEA MAAGLCAGQC ILKVNGSNVM NDGAPEVLEH FQAFRSRREE
 781 ALGLYQWIYH THEDAQEARA SQEASTEDPS GEQAQEEDQA DSAFPLLSLG PRLSLCEDSP
 841 MVTLTVDNVH LEHGVVYEYV STAGVRCHVL EKIVEPRGCF GLTAKILEAF AANDSVFVEN
 901 CRRLMALSSA IVTMPHFEFR NICDTKLESI GQRIACYQEF AAQLKSRVSF PFKQAPLEPH
 961 PLCGLDFCPT NCHINLMEVS YPKTTPSVGR SFSIRFGRKP SLIGLDPEQG HLNPMSYTQH
1021 CITTMAAPSW KCLPAAEGDP QGQGLHDGSF GPASGTLGQE DRGLSFLLKQ EDREIQDAYL
1081 QLFTKLDVAL KEMKQYVTQI NRLLSTITEP TSGGSCDASL AEEASSLPLV SEESEMDRSD
1141 HGGIKKVCFK VAEEDQEDSG HDTMSYRDSY SECNSNRDSV LSYTSVRSNS SYLGSDEMGS
1201 GDELPCDMRI PSDKQDKLHG CLEHLFNQVD SINALLKGPV MSRAFEETKH FPMNHSLQEF
1261 KQKEECTIRG RSLIQISIQE DPWNLPNSIK TLVDNIQRYV EDGKNQLLLA LLKCTDTELQ
1321 LRRDAIFCQA LVAAVCTFSE QLLAALGYRY NNNGEYEESS RDASRKWLEQ VAATGVLLHC
1381 QSLLSPATVK EERTMLEDIW VTLSELDNVT FSFKQLDENY VANTNVFYHI EGSRQALKVI
1441 FYLDSYHFSK LPSRLEGGAS LRLHTALFTK VLENVEGLPS PGSQAAEDLQ QDINAQSLEK
1501 VQQYYRKLRA FYLERSNLPT DASTTAVKID QLIRPINALD ELCRLMKSFV HPKPGAAGSV
1561 GAGLIPISSE LCYRLGACQM VMCGTGMQRS TLSVSLEQAA ILARSHGLLP KCIMQATDIM
1621 RKQGPRVEIL AKNLRVKDQM PQGAPRLYRL CQPPVDGDL
```

C

		Serine (human P-Rex1 numbering)									
		436	805	834	1001	1049	1125	1165	1182	1191	1200
P-Rex1	human	S	S	S	S	S	S	S	S	S	S
	mouse	S	P	S	S	S	S	S	S	S	S
	rat	S	P	S	S	I	S	S	S	S	S
	opossum	S	S	P	S	T	S	S	S	S	S
	platypus	S	D	T	S	S	S	S	S	S	S
	chicken	S	S	I	S	S	P	S	S	S	S
P-Rex2	human	T	K	I	D	-	K	S	S	S	S

Figure S3 MS analysis of P-Rex1

EE–P-Rex1 WT and EE–P-Rex1 VAFA were expressed in PAE cells (without exogenous PP1α) and anti-EE immunoprecipitates subjected to SDS/PAGE. P-Rex1 bands were isolated, digested either with trypsin, chymotrypsin or AspN, and subjected to LC–MS/MS. (**A**) Phosphopeptides and serine phosphorylation sites (bold red) identified in P-Rex1 WT and P-Rex1 VAFA. Mox, methionine sulfoxide. (**B**) A 96 % coverage (residues in red) was achieved and revealed ten phosphoserine residues (highlighted in yellow) both in P-Rex1 WT and P-Rex1 VAFA. The RVxF motif is highlighted in green. (**C**) Conservation of the ten identified phosphoserine sites throughout P-Rex1 evolution. The alignment was performed with ClustalX. Red, conserved residues; blue, fairly conserved residues; green, residues conserved by structural similarity; black, divergent residues.

Received 28 November 2011/10 January 2012; accepted 16 January 2012
Published as BJ Immediate Publication 16 January 2012, doi:10.1042/BJ20112078